The Meteoritical Society

Meteoritics & Planetary Science 53, Nr 11, 2249–2258 (2018)
doi: 10.1111/maps.13121

Cation distribution in orthopyroxenes from São João Nepomuceno iron meteorite inferred from ^{57}Fe Mössbauer spectroscopy: Implications for thermal history and origin of IVA parent body

Edivaldo DOS SANTOS[1*], Rosa B. SCORZELLI[2], and Maria E. VARELA[3]

[1]Instituto de Ciência e Tecnologia—ICT/UFVJM, Rodovia MGT 367—km 583, n° 5000, 39100-000 Minas Gerais, Brazil
[2]Centro Brasileiro de Pesquisas Físicas—CBPF, Rua Dr. Xavier Sigaud 150, 22290-180 Rio de Janeiro, Brazil
[3]Instituto de Ciencias Astronómicas, de la Tierra y del Espacio—ICATE/CONICET, Av España 1512 sur, San Juan, Argentina
[*]Corresponding author. E-mail: edivaldo.santos@ict.ufvjm.edu.br

(Received 11 June 2017; revision accepted 25 April 2018)

Abstract–São João Nepomuceno (SJN) is an IVA iron meteorite, found in Minas Gerais state (Brazil) in 1960, that consists of Fe-Ni metal matrix and coarse-grained silicate inclusions. In spite of the extensive work performed on the IVA irons, there is still no consensus about their origin and thermal history. Their particular chemistry and range in metallographic cooling rates are difficult to explain using conventional models. Furthermore, metal–silicate mixing of the IVA group remains a complex issue. In this work, the ^{57}Fe Mössbauer spectroscopy was applied for measuring the intracrystalline Fe-Mg distribution in orthopyroxenes extracted from SJN. The Mössbauer data associated with Ganguly's cooling rate numerical model were used to investigate the thermal history of SJN meteorite. The results are the background for discussions about the IVA formation models, aiming to improve the understanding of the origin of IVA iron meteorite group.

INTRODUCTION

São João Nepomuceno (SJN) is an IVA iron meteorite, found in Minas Gerais state (Brazil) in 1960, that consists of Fe-Ni metal matrix (81.9 wt%) and coarse-grained silicate inclusions made of tridymite (1.5 wt%), orthopyroxene (12.5 wt%), and low-Ca clinopyroxene (0.8 wt%) (Wasson et al. 2006). As pointed out by Scott et al. (1996), there is still no consensus about the origin and thermal history of IVA irons, if we take into account their particular chemistry and range in metallographic cooling rates. Although IVA irons are extremely depleted in volatile siderophile elements (e.g., Ga, Ge) (Scott et al. 1996), the chemical trends within this group are consistent with an origin in a single metallic body that fractionally crystallized. Nonetheless, their large spread of metallographic cooling rates correlating inversely with Ni content argues against an origin in a mantled asteroidal core (Yang et al. 2007). If this were the case, uniform cooling rates should be expected. Furthermore, metal–silicate mixing of the IVA group remains a complex issue.

As shown in previous works (Ganguly 1982; Kroll et al. 1997), the principal interest concerning the intracrystalline Fe^{2+}-Mg (from now on referred to as Fe-Mg) distribution in orthopyroxene (opx) system is based on its potential application as a tool for retrieving the thermal history of terrestrial and extraterrestrial rocks. Depending on the temperature and pressure history of the host rock, Fe^{2+} and Mg in orthopyroxene crystals fractionate between two nonequivalent octahedral sites, M1 and M2. In slowly cooled crystals, the Fe^{2+} ions populate essentially the M2 position, while Mg ions occupy, predominantly, the M1 position. Conversely, in crystals that have been rapidly cooled, a more disordered Fe-Mg distribution over M1 and M2 sites is observed (Dundon and Hafner 1971).

Here, the intracrystalline Fe-Mg distribution in orthopyroxenes, as measured by means of ^{57}Fe Mössbauer spectroscopy (^{57}Fe-MS), is used to infer the thermal history of SJN meteorite. Ganguly and Stimpfl (2000) have already investigated this thermal history. Nevertheless, we have (at least) three reasons to carry

out the present investigation. First, the present work focuses on powder Mössbauer spectroscopy analysis, while Ganguly and Stimpfl's work is based on single crystal X-ray diffraction (SC-XRD). Since samples are often not available for single crystal experiments, the present work is a straightforward method for investigating the thermal history of meteorites based on cation ordering data. Second, ^{57}Fe-MS is a powerful tool for evaluation of local properties of iron sites. Even though the diffraction method is widespread for site occupancy studies, ^{57}Fe-MS is specifically suitable for iron site occupancy. In addition, ^{57}Fe-MS yields information concerning the oxidation state of such iron atoms, giving a broad picture about any weathering processes suffered by the samples being analyzed. Finally, as shown in previous works (Domeneghetti and Steffen 1992; Skogby et al. 1992; Wang et al. 2005), X-ray diffraction (XRD) and Mössbauer spectroscopy can produce different results for Fe-Mg order–disorder reaction studies in opx. However, as pointed out by Hawthorne (1983), each experimental technique for quantitative characterization of site occupancy in minerals should be viewed as complementary rather than mutually exclusive. Hence, from this point of view, the present work can complement the analysis of Ganguly and Stimpfl (2000).

MATERIALS AND METHODS

Samples

All samples used in this study belong to the Museu Nacional/UFRJ in Rio de Janeiro.

The separation of silicate inclusions of the SJN meteorite from its metallic matrix was done in several thin slices, as described in Dos Santos et al. (2014). The separated grains were inspected under an electron microscope (Jeol JSM 6490 LV, LABNANO-CBPF/MCTIC, Brazil) for verification of their chemical composition. Powdered crystals were used as Mössbauer absorbers.

Electron Microprobe Analysis

Two polished thick sections from SJN were prepared. Under an optical microscope, opx crystals were selected for chemical analysis. Major element chemical compositions were obtained with an ARL-SEMQ (WDS) electron microprobe at ICATE-Argentina, as shown in Dos Santos et al. (2014). Estimated precision for major and minor elements is better than 3% and for Na about 10%. Natural and synthetic standards were used for calibration and an online ZAF correction was applied to the data.

^{57}FE MÖSSBAUER SPECTROSCOPY

^{57}Fe Mössbauer spectroscopy (^{57}Fe-MS), in standard transmission geometry using a 25 mCi ^{57}Co/Rh radioactive source in sinusoidal mode, was performed at temperatures ranging from 25 K to 300 K (±1 K). Spectra were recorded for 24 h in a 512 channel spectrometer and the calibration was taken at room temperature (RT) with an α-Fe foil. The error in source velocity is <1% and the isomer shifts are given relative to α-Fe. The NORMOS code (Brand 1994) was used for the analyses. Mössbauer experiments were carried out at the CBPF (Brazil).

The Fe-Mg intracrystalline distribution measured by Mössbauer spectroscopy is strongly influenced by the thickness effect of the Mössbauer absorber (Greenwood and Gibb 1971). In orthopyroxene, such effect results in an underestimation of the ordering degree. Indeed, Skogby et al. (1992) have shown that an absorber thickness of 5 mg Fe cm^{-2} causes an overestimation of Fe at M1 site by 2%. Therefore, a "thin absorber" is of primary importance for an accurate site occupancy determination. Previous works (Abdu et al. 2009) on clinopyroxenes have shown an agreement between the intracrystalline Fe-Mg distribution inferred from ^{57}Fe-MS with absorbers of 3 mg Fe cm^{-2} and the one inferred from single crystal X-ray diffraction data. That agreement suggests that thickness effects in absorbers of 3 mg Fe cm^{-2} could be negligible and, therefore, they can be considered "thin absorbers." In our work, orthopyroxenes from SJN were prepared as powder absorbers of ~2.0 mg Fe cm^{-2}. As a result, during Mössbauer spectra analysis, thickness effects were considered negligible. Although such proxy is reasonable if the value of 3 mg Fe cm^{-2} is taken as the maximum thickness for a thin absorber in pyroxenes, we cannot exclude that any disagreement between the Mössbauer data presented here and SC-XRD data available in the literature for SJN could be due in part to insufficiently thin Mössbauer absorber.

ORDER–DISORDER REACTION IN ORTHOPYROXENES

Distribution Coefficient and Closure Temperature

The Fe-Mg order–disorder reaction in orthopyroxene can be described by the following intracrystalline exchange reaction (Ghose and Hafner 1967; Mueller 1967; Virgo and Hafner 1969; Ganguly 1982; Zhang 2008):

$$\mathrm{Fe(M2) + Mg(M1) \rightleftharpoons Fe(M1) + Mg(M2)} \qquad (1)$$

where M1 and M2 are the octahedral crystalline sites with slightly different size and symmetry, with M2 being

larger than M1. Since the Mg prefers the M1 site while Fe^{2+} prefers the M2, the forward reaction is the disordering reaction and the backward is the ordering reaction. Considering Fe-Mg as an ideal solution, the intracrystalline distribution of Fe-Mg in reaction 1 can be described by the distribution coefficient (K_D) defined as (Mueller 1967; Ganguly 1982; Zhang 1994, 2008):

$$K_D = \frac{Fe(M1)Mg(M2)}{Fe(M2)Mg(M1)} \quad (2)$$

where Fe(M1) (Fe[M2]) and Mg(M1) (Mg[M2]) are the Fe and Mg occupancies at M1 (M2) sites, respectively. Since the intracrystalline distribution depends on temperature, K_D can be used for determination of the equilibrium (or closure) temperature of reaction 1. The closure temperature of cation ordering is obtained by comparing its quenched ordering state with a calibration (geothermometric equation) of equilibrium ordering versus temperature (Ganguly 1982). Here, the closure temperature will be retrieved from the geothermometric equation of Wang et al. (2005)—calculated based on Mössbauer data of two natural opx single crystals—where the distribution coefficient K_D can be related to the equilibrium temperature T_c in Kelvin by:

$$\ln(K_D) = -\frac{2205}{T_c} + 0.391 \quad (3)$$

Based on Equation 3, Wang et al. (2005) estimated ~18.33 kJ mol^{-1} and ~3.25 J mol^{-1} K^{-1} as the standard enthalpy and entropy changes, respectively, for the intracrystalline exchange equilibrium (1). Several geothermometric equations are available in the literature and most of them are based on SC-XRD data (Ganguly and Stimpfl 2000; Stimpfl et al. 2005). As shown in previous works (Domeneghetti and Steffen 1992; Skogby et al. 1992), the geothermometric equations are not the same when determined by means of SC-XRD or ^{57}Fe-MS, since the distribution coefficient K_D retrieved from both techniques are different. Although these previous works tried to evaluate the reasons for such disagreement, the results were inconclusive. Wang et al. (2005) pointed out that the differences between geothermometric equations (and therefore K_D) retrieved from both techniques mean that ^{57}Fe-MS and SC-XRD equilibrium studies on Fe-Mg order–disorder reactions in opx cannot be mixed. Therefore, since our work is based on Mössbauer spectroscopy, the aforementioned issue justifies the choice of Equation 3 for determination of the equilibrium temperature of the Fe-Mg order–disorder reaction of our samples.

Cooling Rates Inferred From Fe-Mg Intracrystalline Distribution

Based on Mueller's (1967) model for the exchange kinetics of two ions between two nonequivalent lattice sites in quasi-binary crystals, Ganguly (1982) developed a numerical method for determining the cooling rate of opx by measuring its quenched or observed ordering state. Only a brief overview of the method will be given here. First, a cooling path is defined by means of a cooling model (e.g., asymptotic function) with a specific cooling time scale (τ). Then, the cooling history is divided into many time intervals, where the temperature is assumed to be constant. Finally, the reaction progress for each time interval is calculated by solving the reaction rate law for the Fe-Mg intracrystalline distribution between the M1 and M2 sites in the opx structure. After numerically solving the equation, if the final Fe-Mg distribution (i.e., theoretical distribution) does not match the observed ordering state (i.e., the measured distribution), the cooling time scale is changed and the calculation is redone until an agreement between theory and experiment is reached. Once the cooling time scale is defined, the cooling rate for an asymptotic cooling model ($1/T = 1/T_0 + \tau^* t$) is given by $\frac{\partial T}{\partial t} = -\tau T^2$, where τ is a cooling time constant with the dimension of $K^{-1}t^{-1}$ and T is Kelvin. For evaluation of the reaction rate law, we used the forward rate constant (K^+) for the Fe-Mg order–disorder at WI buffer, as determined by Stimpfl et al. (2005):

$$\ln(C_0 K^+) = \frac{41511 - 12600 X_{Fe}}{T(K)} + 28.26 + 5.27 X_{Fe}, \min^{-1} \quad (4)$$

where C_0 represents the total number of M2 + M1 sites occupied by Fe^{2+} and Mg per unit volume of the crystal, X_{Fe} is the bulk atomic fraction of Fe and $T(K)$ is the temperature in Kelvin. It should be pointed out that the numerator of the first term of Equation 4 can be identified as the ratio between the activation energy (Q) for the Fe-Mg order–disorder reaction and the ideal gas constant (R). Stimpfl et al. (2005) determined Equation 4 from SC-XRD experiments in opx crystals extracted from Steinbach (IVA) iron meteorite. Although the distribution coefficient K_D is not the same when determined by means of SC-XRD or ^{57}Fe-MS, as already pointed out (see the Distribution Coefficient and Closure Temperature section), both techniques display a general agreement for K^+. According to Wang et al. (2005), this is in part attributed to the fact that the forward rate constant is a measure of the time scale to reach equilibrium and hence is independent of

Table 1. Electron microprobe average chemical composition (wt%) and unit formula (apfu) for orthopyroxenes from São João Nepomuceno (IVA) meteorite, as shown in Dos Santos et al. (2014).

Chemical composition		Atoms per formula unit (apfu)		
Oxides	Average (wt%)	Elements	Average	±1σ
SiO_2	56.45	Si	1.982	0.009
TiO_2	0.05	^{IV}Al	0.012	0.004
Al_2O_3	0.30	Σ	1.994	
Cr_2O_3	0.64			
FeO	9.29	Ti	0.001	0.001
MnO	0.53	Cr	0.018	0.002
MgO	32.07	Fe^{2+}	0.273	0.005
CaO	0.57	Mn	0.016	0.002
Total	99.90	Mg	1.678	0.014
		Ca	0.021	0.002
		Σ	2.007	

σ = standard deviation

the accurate calibration of the site distribution. It is worth mentioning that the choice of WI buffer is consistent with the chemical data for the SJN meteorite. Indeed, the low Fe/Mn and Fe/Mg ratios of 16 and 0.38, respectively, indicate that SJN crystallized under reducing conditions. Furthermore, the higher Ti/Al ratio of the pyroxenes, as compared to the coexisting tridymite, may signal partitioning behavior of Ti at low oxygen fugacity (Ulff-Moller et al. 1995).

Finally, some consideration concerning the validity of the cooling rate retrieved from the aforementioned numerical method should be raised. As pointed out by Ganguly and Stimpfl (2000), the cooling rate derived from a particular temperature-sensitive property of a mineral is strictly applicable only near the closure temperature of that property. Thus, for the Fe-Mg intracrystalline distribution (a temperature-sensitive property), the cooling rate is valid only near the closure temperature of the Fe-Mg order–disorder reaction for the studied mineral. It is important to mention that near the closure temperature, the calculated cooling rate is not very sensitive to the choice of the cooling model (Ganguly and Stimpfl 2000).

RESULTS

Chemical Composition

The opx average chemical composition (mean of 39 individual analyses) is listed in Table 1, as previously reported in Dos Santos et al. (2014). In terms of the endmembers of pyroxene solid-solution, the studied samples correspond to $En_{85}Fs_{14}Wo_1$. The derived opx unit formula calculated on the basis of six oxygen atoms is given by: $(Fe^{2+}_{0.273}Mg_{1.678}Mn_{0.016}Ca_{0.021}Ti_{0.001}Cr_{0.018})(Si_{1.982},Al_{0.012})O_6$ (Table 1). For estimating the uncertainties (±1σ) shown in Table 1, the unit formula for each individual spot analysis was determined and the average (mean of 39 spots), as well as the associated standard deviation, were computed.

^{57}FE MÖSSBAUER SPECTROSCOPY: 25–300 K

The ^{57}Fe Mössbauer spectra of opx samples, at temperatures ranging from 25 to 300 K, are characterized by two overlapping doublets attributed to Fe^{2+} at two nonequivalent sites (representative spectra are shown in Fig. 1). The first doublet identified as Fe^{2+}(M1), corresponds to Fe^{2+} ions in the less distorted site M1, while the second one, Fe^{2+}(M2), is attributed to Fe^{2+} in the more distorted site M2 (hyperfine parameters are shown in Table 2). Furthermore, all spectra exhibit an asymmetry probably due to texture effects, caused by the preferred orientation of mineral grains, and/or to Goldanskii-Karyagin effect, caused by the anisotropic vibration of the Mössbauer probe (Van Alboom et al. 1993; Wang et al. 2005). The absence of any Fe^{3+} doublets suggests that terrestrial weathering did not take place in these samples. Additionally, Mössbauer spectrum at high velocity (Dos Santos et al. 2014) did not indicate the presence of magnetically ordered iron oxides (e.g., phases related to oxidation processes). Therefore, the minerals in SJN represent a nonaltered assemblage, at least from the latest thermal event that could have affected this meteorite.

Due to the low iron content of our opx samples, the Fe^{2+} quadrupole doublets are highly superimposed and the hyperfine parameters measured at RT are less accurate (Bancroft et al. 1967a, 1967b). Nevertheless, at a given iron concentration, as a result of the differential dependence of the quadrupole splitting on temperature, the resolution of the Fe^{2+}(M1) and Fe^{2+}(M2) doublets increases with decreasing temperature (Srivastava 1986; Van Alboom et al. 1993). In this way, the low temperature range under which ^{57}Fe-MS of our low iron content opx was performed allowed us to reach a better resolution. Therefore, the hyperfine parameters, especially the relative areas that play an important role in Fe site occupancy determination, were obtained at higher accuracy.

The temperature dependence of hyperfine parameters is shown in Fig. 2. In general, the temperature variation of isomer shift (δ), Fig. 2a, is mainly due to the second-order Doppler shift that results from the nonzero mean square velocity of the Mössbauer nucleus. Therefore, this Doppler shift is related to the lattice vibration (Van Alboom et al. 1993; Eeckhout et al. 2000; Chen and Yang 2007). For the quadrupole splitting (Δ), a small temperature dependence is expected when the splitting

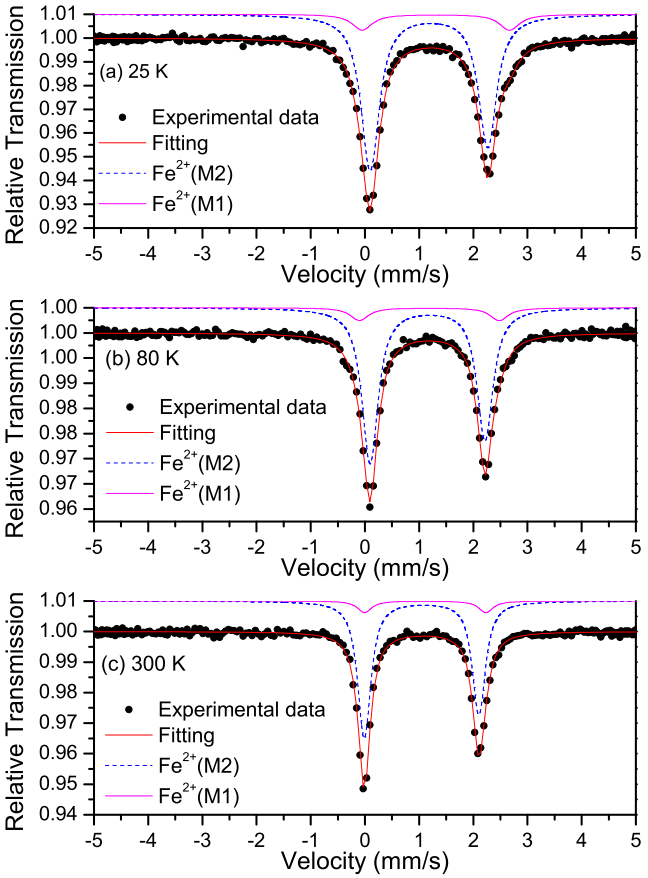

Fig. 1. Representative ^{57}Fe Mössbauer spectra of orthopyroxenes from São João Nepomuceno (IVA) iron meteorite at several temperatures: (a) 25 K, (b) 80K, and (c) 300 K. Fe^{2+}(M1) and Fe^{2+}(M2) stand for Fe^{2+} ions at M1 and M2 orthopyroxene structure sites, respectively. (Color figure can be viewed at wileyonlinelibrary.com.)

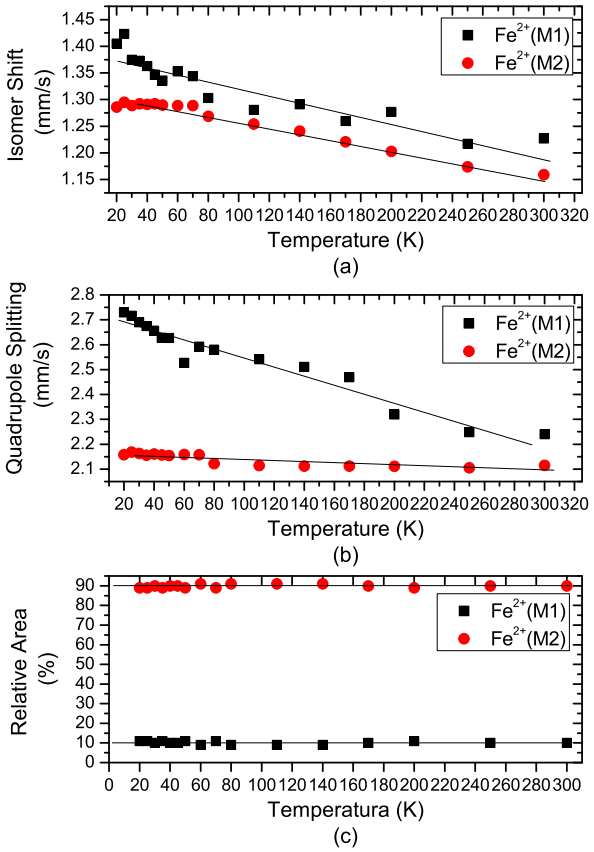

Fig. 2. Temperature dependence of the hyperfine parameters measured in the orthopyroxenes from São João Nepomuceno (IVA) iron meteorite: (a) isomer shift, (b) quadrupole splitting, and (c) relative area. The solid line is just a guide for the eyes. Fe^{2+}(M1) and Fe^{2+}(M2) stand for Fe^{2+} ions at M1 and M2 orthopyroxene structure sites, respectively. (Color figure can be viewed at wileyonlinelibrary.com.)

between *3d* orbitals is larger than the thermal energy, while strong temperature dependence is expected for small splittings (Bancroft 1973; Srivastava 1986). It means that Fe^{2+} ions in regular sites produce a quadrupole splitting that is strongly temperature-dependent, while Fe^{2+} in distorted sites produce small dependencies on temperature. In fact, these observations are in accordance with the trends shown in Fig. 2b for Fe^{2+}(M1) and Fe^{2+}(M2) doublets. In general, the Mössbauer method for determining site population requires the assumption of equality of recoil-free fractions, known also as *f*-factor, that describes the probability of occurrence of the Mössbauer effect. If it is a valid assumption, the area ratio for M1 to M2 sites is expected to be independent of measurement temperature. Indeed, as shown in Fig. 2c, the nearly constant Mössbauer area values for Fe^{2+} at M1 (~10%) and M2 (~90%) sites, with uncertainties close to 0.5%, suggest that the area ratio M1/M2 is independent of temperature measurement. Hence, for the studied samples, the Fe site population will be determined based on the assumption of equality of *f*-factors for Fe^{2+} at M1 and M2. The estimated uncertainties for Mössbauer areas, as shown in Table 2, represents the $\pm 1\sigma$ error limit, and reflects the fitting procedure carried out at temperatures ranging from 25 K to 300 K.

Fe-Mg Order–Disorder Reaction in Orthopyroxenes from SJN: Distribution Coefficient, Closure Temperature, and Cooling Rate

The occupancies of Fe^{2+}(M1) and Fe^{2+}(M2) are obtained by multiplying the Fe^{2+} fractions (i.e., average Mössbauer area) at M1 (10%) and M2 (90%), by the total amount of Fe^{2+} given by electron microprobe results. Thus, $Fe^{2+}(M1) = 0.10 \times 0.273 = 0.027$ and

Table 2. ^{57}Fe Mössbauer hyperfine parameters at 25 to 300 K for orthopyroxenes from São João Nepomuceno (IVA) meteorite. Fe^{2+}(M1) and Fe^{2+}(M2) stand for Fe^{2+} ions at M1 and M2 orthopyroxene structure sites, respectively.

	Fe^{2+} (M1)				Fe^{2+} (M2)			
Temperature (K)	δ (mm s^{-1})	Δ (mm s^{-1})	Γ (mm s^{-1})	A (%)	δ (mm s^{-1})	Δ (mm s^{-1})	Γ (mm s^{-1})	A (%)
25	1.42	2.72	0.44	11	1.30	2.17	0.39	89
30	1.38	2.69	0.45	10	1.29	2.16	0.40	90
35	1.37	2.68	0.43	11	1.29	2.16	0.38	89
40	1.36	2.66	0.44	10	1.29	2.16	0.39	90
45	1.35	2.63	0.42	10	1.29	2.16	0.41	90
50	1.34	2.63	0.40	11	1.29	2.16	0.41	89
60	1.35	2.53	0.40	9	1.29	2.16	0.38	91
70	1.34	2.59	0.41	11	1.29	2.16	0.39	89
80	1.30	2.58	0.39	9	1.27	2.12	0.34	91
110	1.28	2.54	0.39	9	1.25	2.11	0.37	91
140	1.29	2.51	0.39	9	1.24	2.11	0.37	91
170	1.26	2.47	0.40	10	1.22	2.11	0.32	90
200	1.28	2.32	0.36	11	1.20	2.11	0.28	89
250	1.22	2.25	0.37	10	1.17	2.11	0.28	90
300	1.23	2.24	0.30	10	1.16	2.12	0.27	90

δ = isomer shift relative to alpha iron (±0.01 mm s^{-1}).
Δ = quadrupole splitting (±0.01 mm s^{-1}); A: relative area (±0.5%).
Γ = line width (±0.05 mm s^{-1}).

$Fe^{2+}(M2) = 0.90 \times 0.273 = 0.246$. Assuming complete order of Cr and Ti atoms at M1 site and Mn and Ca atoms at M2 site (Wang et al. 2005), the occupancy of Mg at M1 and M2 sites can be calculated as follows: $Mg(M1) = 1 - (Fe^{2+}(M1) + N_{Cr} + N_{Ti}) = 0.954$ and $Mg(M2) = N_{Mg} - Mg(M1) = 0.724$, where N_{Cr}, N_{Ti}, N_{Mg} are the numbers of Cr, Ti, and Mg atoms per formula unit. Hence, from Equation 2, the distribution coefficient for the studied sample is $K_D = 0.083$. Using the geothermometric calibration of Wang et al. (2005) (see Equation 3), we found $T_c = (497 \pm 20)$ °C for the closure temperature of the order–disorder reaction in the opx from SJN meteorite. Table 3 shows the occupancy data along with their respective uncertainties (±1σ) that arise from the error propagation for standard deviations of both microprobe analysis and the Mössbauer data.

Table 3. Summary of occupancy data, coefficient distribution (K_D), closure temperature (T_C), and cooling rate (CR) for the orthopyroxene (opx) extracted from São João Nepomuceno (SJN) iron meteorite. The numbers within parentheses are the estimated standard deviations. The uncertainties of Mössbauer relative area and microprobe analysis leads to uncertainty factor of ~10^2 for orthopyroxene cooling rates.

M1-site	
Fe^{2+}	0.027 (2)
Mg	0.954 (5)
Cr	0.018 (2)
Ti	0.001 (1)
M2-site	
Fe^{2+}	0.246 (5)
Mg	0.724 (019)
Mn	0.016 (2)
Ca	0.021 (2)
T-site	
Si	1.982 (9)
Al	0.012 (4)
K_D	0.083 (6)
T_C (°C)	497
CR (°C Myr^{-1})	10,400

Taking into account the thermodynamic parameters (standards enthalpy/entropy and activation energy) for the Fe-Mg order–disorder reaction inferred from Equations 3 and 4, Ganguly's cooling rate method applied to the opx samples from SJN meteorite yields ~10,400 °C Myr^{-1} as cooling rate. Considering the uncertainties of Mössbauer relative area and microprobe analysis, error propagation for the observed iron fraction at M2 site leads to uncertainty factor of ~10^2 for orthopyroxene cooling rates. The order–disorder reaction progress in orthopyroxene (i.e., the changes of Fe fraction at M2 site) over the cooling path around the closure temperature of ~500 °C, for the sample investigated in this work along with three different samples (SJN23, SJN24, and SJN25) studied by Ganguly and Stimpfl (2000), is shown in Fig. 3.

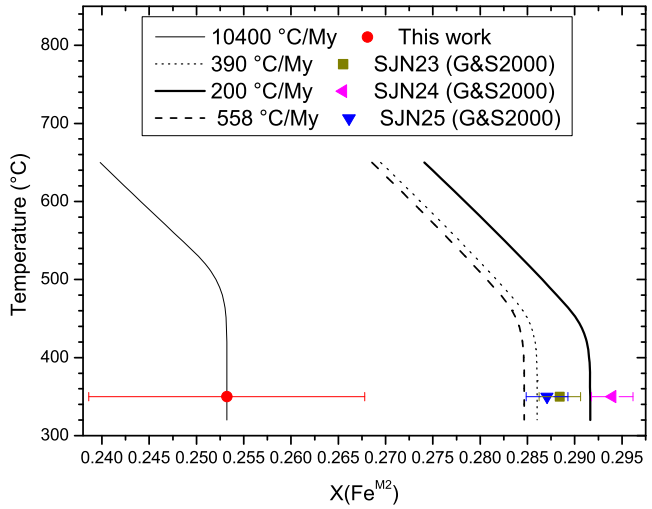

Fig. 3. Numerical simulation for the evolution of iron fraction at M2 site (i.e., X[Fe^{M2}]) versus temperature. *Circle*: site occupancy observed in this work. *Square, left and right triangles*: site occupancy measured by G&S2000 (Ganguly and Stimpfl 2000) for SJN23, SJN24, and SJN25 samples, respectively. Error bars: ±1σ. X(Fe^{M2}) = Fe(M2)/(Fe[M2]+Mg[M2]), where Fe(M2) and Mg(M2) are the iron and magnesium occupancies at M2 site. (Color figure can be viewed at wileyonlinelibrary.com.)

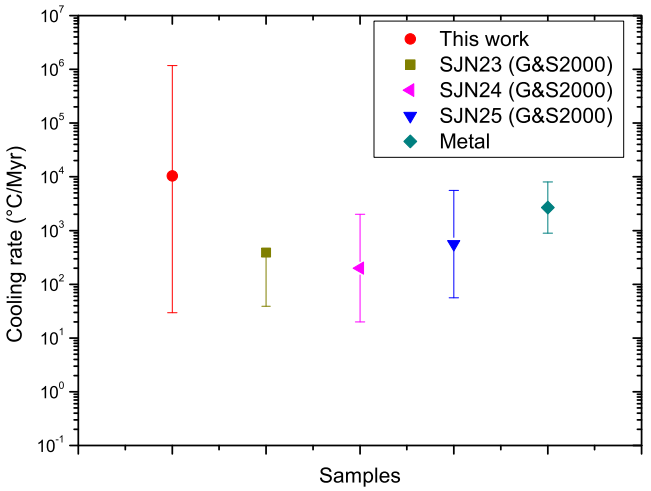

Fig. 4. Comparison of the cooling rates at ~400–500 °C derived from the Fe-Mg ordering studies in orthopyroxenes with those derived from the metallographic data in São João Nepomuceno. *Circle*: site occupancy observed in this work. *Square, left and right triangles*: site occupancy measured by G&S2000 (Ganguly and Stimpfl 2000) for SJN23, SJN24, and SJN25 samples, respectively. *Diamond*: metallographic data (see text for details). Error bars: ±1σ. (Color figure can be viewed at wileyonlinelibrary.com.)

DISCUSSION

Thermal History and Origin of IVA Irons

In this work, it was found that orthopyroxene crystals extracted from SJN meteorite experienced cooling rates of ~10,400 °C Myr^{-1} at temperatures close to T_c (~500 °C). However, at temperatures near 1200 °C, previous works suggest a fast cooling of silicates found in SJN. According to Haack et al. (1996) and Ruzicka and Hutson (2006), the clinobronzites found in SJN were formed by inversion during rapid cooling (~100 °C h^{-1}) of protobronzite at high temperatures (~1200 °C). Therefore, the evidence of rapid cooling on one hand, and of slow cooling for opx samples (~10,400 °C Myr^{-1}, this work) on the other, suggests that the thermal history of silicates from SJN suffered a drastic change. This view is in accordance with oxygen isotopic composition studies of silicate inclusions in IVA irons that indicates decreasing of cooling rates at temperatures below 1200 °C (Wang et al. 2004). Ganguly and Stimpfl (2000) also investigated the thermal history of SJN iron meteorite. Applying X-ray diffraction for opx cation ordering studies in SJN, Ganguly and Stimpfl (2000) retrieved an average closure/equilibrium temperature of 400 °C and cooling rate ranging ~200–560 °C Myr^{-1}. Considering that silicates in SJN experienced rapid cooling at high temperatures, as pointed out by Haack et al. (1996) and Ruzicka and Hutson (2006), the results of Ganguly and Stimpfl (2000) also indicate drastic changes in cooling rates for opx from SJN. Therefore, the thermal history of silicates presented in this work reinforces the analysis of Ganguly and Stimpfl (2000). Although the cooling rate value (~10,400 °C Myr^{-1}) found in our work is a factor of ~19–52 higher than Ganguly's result for SJN, both results are compatible if the ±1σ error limit is considered (Fig. 4). The difference between the cooling rate found in our work (based on Mössbauer data) and the one reported by Ganguly and Stimpfl (2000), based on X-ray diffraction, mainly arises from the differences in site occupancy data. As already pointed out (see the ^{57}Fe Mössbauer Spectroscopy section), insufficiently thin Mössbauer absorber overestimates the amount of Fe at M1 site by 2%; as a result, XRD gives a more ordered Fe-Mg distribution than Mössbauer spectroscopy. Additionally, the partition method adopted by Ganguly and Stimpfl (2000), where Fe^{2+} and Mn are considered as one species, has implications for the determination of cooling rates based on ordering state of orthopyroxene, mainly for the low Fe samples. Indeed, Stimpfl (2005) showed that the calculated cooling rate, for low Fe opx samples, increases by 350% when Fe is partitioned independently from Mn. Hence, it follows from the work of Stimpfl (2005) that the practice of partitioning Fe^{2+} and Mn as one species overestimates the amount of Fe at M2 site.

The cooling rate of the metallic fraction of SJN should be analyzed. According to Rasmussen et al. (1995), at temperature range ~350–650 °C where the Widmanstätten pattern formed, the metallographic cooling rate for SJN is 890 °C Myr^{-1} with uncertainty better than a factor of 3. However, Yang et al. (2008) reviewed the cooling rate data for 13 IVA iron meteorites and concluded that the cooling rates determined by Rasmussen et al. (1995) are about three times lower. Therefore, in our work, the metallographic cooling rate for SJN will be the one measured by Rasmussen et al. (1995) multiplied by a factor of 3, i.e., ~2670 °C Myr^{-1}. Indeed, as pointed out by Dos Santos et al. (2015), the evidence of disordered taenite in metal fractions of SJN is consistent with cooling rates close to 2670 °C Myr^{-1}.

Origin of IVA Irons

The chemical properties of IVA irons suggest that they represent samples from metallic cores that fractionally crystallized (Scott et al. 1996). However, this view has several problems. (1) Two IVA members (SJN and Steinbach) contain huge amounts of silicates; (2) the wide range of metallographic cooling rates for IVA iron correlating inversely[1] with Ni content argues against an origin in a mantled asteroidal core; (3) depletion of volatile siderophile elements is not consistent with fractional crystallization (e.g., Wasson et al. 2006). Notwithstanding the constant efforts devoted to clarify these issues, it should be noted that any model concerning the origin of IVA iron meteorites should take into account not only the chemistry and the complex thermal history of such samples but also the petrology, texture, and mineralogy (e.g., see the review on IVA formation models in Ruzicka 2014). In the following paragraphs, we summarized three of such models: the breakup/reassembly model of Haack et al. (1996), the model of Ganguly and Stimpfl (2000), and the unified model of Ruzicka and Hutson (2006).

The breakup/reassembly model can be described in four stages, as follows. (1) Igneous evolution of the IVA parent body with differentiation into mantle, core, and crust; (2) breakup and reassembly; (3) thermal equilibration of hot and cold reassembled fragments, providing the wide cooling rate range for the IVA irons; and (4) dispersal of the reassembled material. One of the major difficulties of this model is that it cannot explain the strong correlation between cooling rates and Ni content (Wasson et al. 2006). Indeed, in order to establish such a correlation, Ni-rich and Ni-poor metal produced in the first body should be put into the correct location inside the second body (Ruzicka 2014).

Considering the orthopyroxene cation ordering data and the metallographic cooling rates for SJN and Steinbach meteorites, Ganguly and Stimpfl (2000) argued for a single parent body model for the high and low Ni IVA irons. According to this model, SJN (low Ni) and Steinbach (high Ni) IVA iron meteorites experienced fast cooling at high temperature, at a similar rate of ~400 °C Myr^{-1}, after the gravitational reassembly of the disrupted parent body created a random mixture of metal and silicate, as pictured by Haack et al. (1996). Then, Steinbach and SJN experienced slow cooling (~50 °C Myr^{-1}) at 425 °C and <350 °C, respectively. In the framework of Ganguly and Stimpfl's model, similar cooling rates for SJN and Steinbach, at high temperature, are mandatory to make compatible the metallographic and opx cooling rate data for both samples. Therefore, this model (as well as the breakup/reassembly model of Haack) did not support the idea of different cooling rates for high and low Ni IVA irons. According to Ganguly and Stimpfl (2000), the correlation between cooling rate and Ni content of the IVA irons is at variance with the orthopyroxene cation ordering data for SJN and Steinbach. Additionally, in a pilot study about the distribution of Co between kamacite and taenite to infer relative cooling rates of iron meteorites, Wasson and Hoppe (2012) argued that the large cooling rate range in IVA irons, inferred by Rasmussen et al. (1995) and Yang et al. (2008), is inconsistent.

The unified model of Ruzicka and Hutson (2006) involves endogenic heating and collisional disruption. In this model, the IVA parent body was substantially molten and differentiated. The core was mostly molten and the mantle was roughly composed of equal portions of olivine and silicate melt. Due to an ulterior collision, the mantle might have been removed and the exposed core solidified inwards as a largely metallic body. This gave rise to the IVA irons without silicate inclusions. But such an impact could also promote the injection of some of the mantle-derived silicates into the molten core (Ruzicka and Hutson 2006) favoring the formation of IVA irons with silicate inclusions.

The unified model appears to overcome many of the issues concerning the origin of IVA irons. First, the texture/petrology of SJN and Steinbach indicates that coarse-grained Si-rich orthopyroxenite assemblages formed by incorporation of silicate clusters in a metallic melt (Scott et al. 1996; Ruzicka and Hutson 2006; Wasson et al. 2006). Since silicate will separate from

[1]Several authors (e.g., Ganguly and Stimpfl 2000; Wasson and Hoppe 2012) have questioned the inverse correlation between cooling rate and Ni content of the IVA irons. Nevertheless, Goldstein et al. (2014) and Yang et al. (2007, 2008) have shown that the cooling rate range observed in a metallic body with negligible silicate mantle matches the inverse correlation found in the IVA irons.

metal on a short time scale due to buoyancy, a rapid cooling to avoid metal–silicate separation should follow metal–silicate mixing. Indeed, the clinobronzites found in SJN and Steinbach point toward a fast cooling process at high temperatures (~1200 °C) (Haack et al. 1996; Ruzicka and Hutson 2006). Second, the metallic body without silicate insulation could span the cooling rate range observed in the IVA irons. A metallic body of 150 ± 50 km in radius with negligible silicate mantle (<1 km) exhibits a cooling rate range that matches the metallographic cooling rates and Ni composition correlation found in the IVA irons (Yang et al. 2007, 2008). Such a metallic body would crystallize inwards with the lowest-Ni irons forming first on the outside. Also, the depletion of volatile siderophile elements (e.g., Ga and Ge) may have occurred due to vaporization of such elements when the hot metallic core was exposed to a vacuum during impact disruption (Ruzicka 2014). Then, the question that arises is how to reconcile (if possible) the thermal history of silicates and metal at low temperatures with the unified model? The answer is not straightforward. Since silicates and metal cool in the same environment, they are supposed to experience similar cooling rates. Nevertheless, in the framework of our results, this is only possible if the uncertainty factor ($\sim 10^2$) for opx cooling rate is considered. Then, the estimated cooling rate around T_c for opx from SJN (~10,400 °C Myr^{-1}) can range from $\sim 10^2$ up to $\sim 10^6$ °C Myr^{-1}. Given that the metallographic cooling rate for SJN (~2670 °C Myr^{-1}) falls into the opx cooling rate range, we can suggest that both silicates and metal experience similar thermal history at low temperatures (see Fig. 4). It is worth mentioning that such result is compatible with the analysis of Ganguly and Stimpfl (2000).

CONCLUSION

The intracrystalline Fe-Mg distribution in orthopyroxenes measured by means of ^{57}Fe Mössbauer spectroscopy was used to infer the thermal history of SJN meteorite. Our results appear to be consistent with the unified model of Ruzicka and Hutson (2006) that involves endogenic heating/collisional disruption and explains the metallographic cooling rates and Ni composition correlation found in the IVA irons (Rasmussen et al. 1995; Yang et al. 2008; Goldstein et al. 2014). In contrast, many authors have questioned such correlation (Ganguly and Stimpfl 2000; Wasson and Hoppe 2012). If the metallographic cooling rate correlation found in IVA irons is an artifact of measurement, as argued by Wasson and Hoppe (2012), the single body model of Ganguly and Stimpfl (2000) represents an alternative interpretation for the origin of IVA irons. However, and considering that our work focused only on SJN meteorite, and taking into account that both the works are based on different experimental techniques (X-ray diffraction and Mössbauer spectroscopy), our results should be seen as complementary, and therefore not fully comparable, to those presented by Ganguly and Stimpfl (2000), where SJN and Steinbach samples were studied.

In order to get closer to an answer concerning the IVA origin, we are convinced that it is extremely important to unify criteria and get an agreement about the involved methods to determine the orthopyroxene and metallographic cooling rates. In addition, the precision and accuracy of the involved methods for cooling rate calculation need to be improved.

Acknowledgments—Cooling rate calculation was made possible thanks to the template provided by Prof. Jibamitra Ganguly. The authors are also grateful to LABNANO/CBPF for technical support during electron microscopy work and M. E. Zucolotto (Museu Nacional/UFRJ) for providing São João Nepomuceno samples. R. B. Scorzelli acknowledges financial support from FAPERJ and CNPq. E. dos Santos acknowledges financial support from FAPEMIG. M. E. Varela acknowledges financial support from PIP 1645 (CONICET) and CNPQ during scientific visits to CBPF. Constructive reviews from John Willis, Jibamitra Ganguly, and Alex Ruzicka (Associate Editor) helped to considerably improve the manuscript.

Editorial Handling—Prof. Alex Ruzicka

REFERENCES

Abdu Y. A., Scorzelli R. B., Varela M. E., Kurat G., Azevedo I. S., Stewart S. J., and Hawthorne F. C. 2009. Druse clinopyroxene in D'Orbigny angritic meteorite studied by single-crystal X-ray diffraction, electron microprobe analysis, and Mössbauer spectroscopy. *Meteoritics & Planetary Science* 44:581–587.

Bancroft G. M. 1973. *Mössbauer spectroscopy: an introduction for inorganic chemist and geochemists*. London: McGraw-Hill Book Company. 252 p.

Bancroft G. M., Burns R. G., and Howie R. A. 1967a. Determination of the cation distribution in the orthopyroxene series by the Mössbauer effect. *Nature* 25:1221–1223.

Bancroft G. M., Maddock A. G., and Burns R. G. 1967b. Applications of the Mössbauer effect to silicate mineralogy —I. Iron silicates of known crystal structure. *Geochimica et Cosmochimica Acta* 31:2219–2246.

Brand R. A. 1994. *Normos-90: Mössbauer fitting package user's guide*. Duisburg, Germany: Universität Duisburg.

Chen Y. and Yang D-P. 2007. *Mössbauer effect in lattice dynamics*. Weinheim, Germany: Wiley-VCH Verlag GmbH & Co., KGaA. 423 p.

Domeneghetti M. C. and Steffen G. 1992. M1, M2 site populations and distortion parameters in synthetic Mg-Fe orthopyroxenes from Mössbauer spectra and X-ray structure refinements. *Physics and Chemistry of Minerals* 19:298–306.

Dos Santos E., Scorzelli R. B., Varela M. E., and Munayco P. 2014. Fe^{2+}-Mg order-disorder study in orthopyroxenes from São João Nepomuceno (IVA) iron meteorite. *Hyperfine Interactions* 224:251–256.

Dos Santos E., Gattacceca J., Rochette P., Scorzelli R. B., and Fillion G. 2015. Magnetic hysteresis properties and ^{57}Fe Mössbauer spectroscopy of iron and stony-iron meteorites: Implications for mineralogy and thermal history. *Physics of the Earth and Planetary Interiors* 242:50–64.

Dundon R. W. and Hafner S. S. 1971. Cation disorder in shocked orthopyroxene. *Science* 174:581–583.

Eeckhout S. G., De Grave E., McCammon C. A., and Vochten R. 2000. Temperature dependence of the hyperfine parameters of synthetic $P2_1/c$ Mg-Fe clinopyroxenes along $MgSiO_3$-$FeSiO_3$ join. *American Mineralogist* 85:943–952.

Ganguly J. 1982. Mg-Fe order-disorder in ferromagnesian silicates: II. Thermodynamics, kinetics and geological applications. *Advances in Physical Geochemistry* 2:58–99.

Ganguly J. and Stimpfl M. 2000. Cation ordering in orthopyroxenes from two stony-iron meteorites: Implications for cooling rates and metal-silicate mixing. *Geochimica et Cosmochimica Acta* 64:1291–1297.

Ghose S. and Hafner S. 1967. Mg^{2+}-Fe^{2+} distribution in metamorphic and volcanic orthopyroxenes. *Zeitschrift für Kristallographie*. 125:1–6.

Goldstein J., Yang J., and Scott R. D. 2014. Determining cooling rates of iron and stony-iron meteorites from measurements of Ni and Co at kamacite-taenite interfaces. *Geochimica et Cosmochimica Acta* 140:297–320.

Greenwood N. N. and Gibb T. C. 1971. *Mössbauer spectroscopy*. London: Chapman and Hall Ltd. 330 p.

Haack H., Scott E. R. D., Love S. G., Brearley A. J., and McCoy T. J. 1996. Thermal histories of IVA stony-iron meteorites: Evidence for asteroid fragmentation and reaccretion. *Geochimica et Cosmochimica Acta* 60:3103–3113.

Hawthorne F. C. 1983. Quantitative characterization of site-occupancies in minerals. *American Mineralogist* 68:287–306.

Kroll H., Lueder T., Schlenz H., Kirfel A., and Vad T. 1997. The Fe^{2+}-Mg distribution in orthopyroxene: A critical assessment of its potential as geospeedometer. *European Journal of Mineralogy* 9:733–750.

Mueller R. F. 1967. Model for order-disorder kinetics in certain quasi-binary crystals of continuously variable composition. *Journal of Physics and Chemistry of Solids* 28:2239–2243.

Rasmussen K. L., Ulff-Moller F., and Haack H. 1995. The thermal evolution of IVA iron meteorites: Evidence from metallographic cooling rates. *Geochimica et Cosmochimica Acta* 59:3049–3059.

Ruzicka A. 2014. Silicate-bearing iron meteorites and their implications for the evolution of asteroidal parent bodies. *Chemie der Erde Geochemistry* 74:3–48.

Ruzicka A. and Hutson M. 2006. Differentiation and evolution of the IVA meteorite parent body: Clues from pyroxene geochemistry in the Steinbach stony-iron meteorite. *Meteoritics & Planetary Science* 41:1959–1987.

Scott E. R. D., Haack H., and McCoy T. J. 1996. Core crystallization and silicate-metal mixing in the parent body of the IVA iron and stony-iron meteorites. *Geochimica et Cosmochimica Acta* 60:1615–1631.

Skogby H., Annersten H., Domeneghetti M. \C., Molin G. M., and Tazzoli V. 1992. Iron distribution in orthopyroxene: A comparison of Mössbauer spectroscopy and X-ray refinement results. *European Journal of Mineralogy* 4:441–452.

Srivastava K. K. P. 1986. Electronic spin relaxation in Mössbauer spectra of Fe^{2+} in mineral hypersthene. *Journal of Physics C: Solid State Physics* 19:6407–6416.

Stimpfl M. 2005. The Mn, Mg-intracrystalline exchange reaction in donpeacorite ($Mn_{0.54}Ca_{0.03}Mg_{1.43}Si_2O_6$) and its relation to the fraction behavior of Mn in Fe, Mg-orthopyroxene. *American Mineralogist* 90:155–161.

Stimpfl M., Ganguly J., and Molin G. 2005. Kinetics of Fe^{2+}-Mg order-disorder in orthopyroxene: Experimental studies and applications to cooling rates of rocks. *Contributions to Mineralogy and Petrology* 150:319–334.

Ulff-Moller F., Rasmussen K. L., Kallemeyn G. W., Prinz M., Palme E. H., and Spettel B. 1995. Differentiation of the IVA parent body: Evidence from silicate-bearing iron meteorites. *Geochimica et Cosmochimica Acta* 59:4713–4728.

Van Alboom A., De Grave E., and Vandenberghe R. E. 1993. Study of the temperature dependence of the hyperfine parameters in two orthopyroxenes by ^{57}Fe Mössbauer spectroscopy. *Physics and Chemistry of Minerals* 20:263–275.

Virgo D. and Hafner S. S. 1969. Fe^{2+}, Mg order-disorder in heated orthopyroxenes. *Mineralogical Society of America Special Paper* 2:67–81.

Wang P. L., Rumble D., and McCoy T. J. 2004. Oxygen isotopic compositions of IVA iron meteorites: Implications for the thermal evolution derived from in situ ultraviolet laser microprobe analyses. *Geochimica et Cosmochimica Acta* 68:1159–1171.

Wang L., Moon N., Zhang Y., Dunham W. R., and Essene E. J 2005. Fe-Mg order-disorder in orthopyroxenes. *Geochimica et Cosmochimica Acta* 69:5777–5788.

Wasson J. T. and Hoppe J. 2012. Co/Ni ratios at taenite/kamacite interfaces and relative cooling rates in iron meteorites. *Geochimica et Cosmochimica Acta* 84:508–524.

Wasson J. T., Matsunami Y., and Rubin A. 2006. Silica and pyroxene in IVA irons: Possible formation of the IVA magma by impact melting and reduction of L-LL chondrite materials followed by crystallization and cooling. *Geochimica et Cosmochimica Acta* 70:3149–3172.

Yang J., Goldstein J. I., and Scott E. R. D. 2007. Iron meteorite evidence for early formation and catastrophic disruption of protoplanets. *Nature* 446:888–891.

Yang J., Goldstein J. I., and Scott E. R. D. 2008. Metallographic cooling rates and origin of IVA iron meteorites. *Geochimica et Cosmochimica Acta* 72:3043–3061.

Zhang Y. 1994. Reaction kinetics, geospeedometry, and relaxation theory. *Earth and Planetary Science Letters* 122:373–391.

Zhang Y. 2008. *Geochemical kinetics*. United Kingdom: Princeton University Press. 664 p.